

# Magnetite NPs@C with Highly-Efficient Peroxidase-Like Catalytic Activity as an Improved Biosensing Strategy for Selective Glucose Detection

Mercedes Arana,<sup>[b]</sup> Cecilia S. Tettamanti,<sup>[a]</sup> Paula G. Bercoff,<sup>[b]</sup> and Marcela C. Rodríguez<sup>\*[a]</sup>

**Abstract:** This work reports the novel application of carbon-coated magnetite nanoparticles (mNPs@C) as catalytic nanomaterial included in a composite electrode material (mNPs@C/CPE) taking advantages of their intrinsic peroxidase-like activity. The nanostructured electrochemical transducer reveals an enhancement of the charge transfer for redox processes involving hydrogen peroxide. Likewise, mNPs@C/CPE demonstrated to be highly selective even at elevated concentrations of ascorbic acid and uric acid, the usual interferents of blood glucose analysis. Upon these remarkable results, the composite matrix was further modified by the addition of glucose oxidase as

biocatalyst, in order to obtain a biosensing strategy (GOx/mNPs@C/CPE) with enhanced properties for the electrochemical detection of glucose. GOx/mNPs@C/CPE exhibit a linear range up to  $7.5 \times 10^{-3} \text{ mol L}^{-1}$  glucose, comprising the entirely physiological range and incipient pathological values. The average sensitivity obtained at  $-0.100 \text{ V}$  was  $(1.62 \pm 0.05) \times 10^5 \text{ nA L mol}^{-1}$  ( $R^2 = 0.9992$ ), the detection limit was  $2.0 \times 10^{-6} \text{ M}$  while the quantification limit was  $6.1 \times 10^{-6} \text{ mol L}^{-1}$ . The nanostructured biosensor demonstrated to have an excellent performance for glucose detection in human blood serum even for pathological values.

**Keywords:** Carbon-coated magnetite nanoparticles • Electrochemical glucose biosensor • Glucose oxidase • Modified-carbon paste electrode • Peroxidase-like activity

## 1 Introduction

Nowadays, there is a rising demand for powerful analytical tools with high sensitivity and reliability, fast response, excellent selectivity, accuracy and low cost [1–3]. In particular, biosensors have found versatile applications in the field of environmental control, hazard material detection, pharmaceuticals and clinical diagnostics [4–6]. Therefore, the main goal in biosensors development is the successful construction of a biospecific surface, highly sensitive and selective for a particular analyte, that can generate detectable signals coupled to a suitable transducer (electrochemical, optical, piezoelectrical, thermal, among others) [7].


A number of different nanomaterials offer outstanding properties, such as fast electron transfer kinetics, high surface-to-volume ratio, excellent biocompatibility, chemical stability and the possibility of easy biomolecular coupling [2,5,8]. Hence, nanomaterials have been employed in the design of biofunctional surfaces in order to boost the biorecognition event and the signal transduction [7]. Likewise, several kinds of nanomaterials exhibit enzyme-like activity in a wide range of nonphysiological conditions such as extreme pH values, high temperature or in the presence of inhibitors [9]. This type of functional nanomaterials, that could be named “artificial enzymes”, has attracted great attention in the last years due to several advantages, namely stability under harsh conditions and effective biocatalysis as replacement of natural enzymes. Even though magnetic nanoparticles with different com-

positions, sizes and shapes have been developed for biomedical applications, the most frequently used magnetic materials are maghemite ( $\gamma\text{-Fe}_2\text{O}_3$ ) and magnetite ( $\text{Fe}_3\text{O}_4$ ) [10–15]. In this sense, magnetite nanoparticles (NPs) have demonstrated intrinsic peroxidase-like activity and have been applied as peroxidase nanomimetics to detect a wide range of biomolecules [16–22].

For over 50 years [23], glucose biosensors have been the classic icon in the development of biosensors [24,25]. The main challenge when designing electrochemical glucose biosensors using carbon electrodes is the development of strategies that allow an important decrease in the high overvoltage required for the oxidation of hydrogen peroxide in order to improve glucose quantification under highly selective conditions [26]. Comba et al [26–28] reported the advantages of carbon paste electrodes (CPE) modified with magnetite and iron NPs in glucose biosensors. Though sensor sensitivity increases with the

[a] C. S. Tettamanti, M. C. Rodríguez  
Departamento de Físicoquímica, Facultad de Ciencias Químicas, Universidad Nacional de Córdoba  
INFIQC, CONICET, Córdoba, Argentina  
phone: +54-351-5353866 ext: 53567; fax: +54-351-4334188  
\*e-mail: marcela.rodriguez@fcq.unc.edu.ar

[b] M. Arana, P. G. Bercoff  
Facultad de Matemática, Astronomía y Física, Universidad Nacional de Córdoba  
IFEG, CONICET, Córdoba, Argentina

 Supporting Information for this article is available on the WWW under <http://dx.doi.org/10.1002/elan.201400159>.

amount of magnetite, high NPs contents promote a highly resistive behavior due to the low-conductive nature of magnetite. It was found that shape and structure of magnetite NPs influence the peroxidase-nanomimetics catalytic activity, which is closely related to the exposed active iron atoms or crystal planes of the NPs [29]. Moreover, particles interfaces are bound to play an important role in any sensor response. In fact, different modifications of magnetite NPs have been proposed in order to improve their catalytic activity. Both organic [30,31] and inorganic [32–34] compounds have been proposed for different catalytic reactions, obtaining favorable results in every case. However, to our knowledge, carbon-covered nanoparticles have never been studied for this application.

In this work, we propose for the first time the use of carbon-coated magnetite NPs (mNPs@C) as catalytic nanomaterial, taking advantage of their peroxidase-like activity. The mNPs@C were prepared by mechanosynthesis and their structural and magnetic characterization has previously been reported [35]. In the following sections, we explore the peroxidase-like catalytic activity of carbon paste electrodes (CPE) modified with mNPs@C (mNPs@C/CPE) towards hydrogen peroxide and its applicability as a nanostructured-responsive biosurface for highly sensitive and selective glucose detection.

## 2 Experimental

### 2.1 Reagents

Hydrogen peroxide (30% v/v aqueous solution), glucose and uric acid were purchased from Merck while ascorbic acid,  $\text{Na}_2\text{HPO}_4$  and  $\text{NaH}_2\text{PO}_4$  were provided by Baker. Glucose oxidase (GOx) (Type X-S, *Aspergillus niger*, (EC 1.1.3.4), 158,900 units per gram of solid, catalog number G-7141) was obtained from Sigma. Standatrol S-E-2 (Lot # 1202085070), Level N1 (# 085070) and Level N2 (# 085070) was obtained from Wiener Lab. Mineral oil was purchased from Aldrich while graphite powder (grade 38) was acquired from Fischer Scientific. Commercial magnetite microparticles (0.5–1.0  $\mu\text{m}$ ) were provided by Strem Chemicals. Ultrapure water ( $\rho=18\text{ M}\Omega$ ) from a Millipore-MilliQ system was used for preparing all the solutions. A 0.050 molL<sup>-1</sup> phosphate buffer solution (pH 7.40) was used as supporting electrolyte. Other chemicals were reagent grade and used without further purification.

### 2.2 Apparatus

The electrochemical measurements were performed with a TEQ 04 potentiostat. The electrodes were inserted into the cell (BAS, Model MF-1084) through holes in its Teflon cover. A platinum wire and Ag/AgCl, 3 molL<sup>-1</sup> KCl (BAS, Model RE-5B) were used as counter and reference electrodes, respectively. All potentials are referred to the latter. A magnetic stirrer provided the convective transport during the amperometric measurements.

### 2.3 Synthesis of mNPs@C

mNPs@C were synthesized according to the method previously described [35]. Briefly, mNPs@C were obtained by the mechanochemical method in a Fritsch Pulverisette 7 high-energy ball mill by reduction of the precursors hematite and amorphous carbon. The milling was performed at 700 rpm, with a ball/powder mass ratio of 35, in stainless steel vials with WC balls under Ar atmosphere. The precursor powder was milled for 18 hours and annealed for 2 h in Ar at 500 °C. The structural and magnetic characterization of the system was performed by different techniques as it is reported in [35].

### 2.4 Preparation of the Working Electrodes

The electrochemical characterization of mNPs@C was performed using a composite carbon paste electrode (CPE). The CPE was prepared in a regular way by mechanically mixing graphite powder (70.0% w/w) and mineral oil (30.0% w/w) in an agate mortar for 30 min. CPEs containing mNPs@C (mNPs@C/CPE) and commercial magnetite microparticles (0.5–1.0  $\mu\text{m}$ ) (MPs/CPE) were prepared in a similar way, mixing first the mNPs@C or commercial magnetite MPs with mineral oil for 3 min, followed by the incorporation of the graphite powder and mixing for additional 30 min. In the case of the enzymatic electrode, GOx and mNPs@C were first mixed with the mineral oil for 10 min before incorporating the graphite powder and then mixed for additional 30 min. A portion of the resulting paste was packed firmly into the cavity of a Teflon tube (3 mm diameter). The electric contact was established through a stainless steel screw. A new surface was obtained by smoothing the electrode onto a weighing paper before starting every new experiment. Cyclic voltammetry experiments were performed in 0.050 M buffer phosphate solution pH 7.40 as supporting electrolyte. The amperometric measurements were conducted in a stirred 0.050 molL<sup>-1</sup> buffer phosphate solution pH 7.40 by applying the desired working potential and allowing the transient current to decay to a steady-state prior to the addition of the analyte and subsequent current monitoring. All the electrochemical measurements were performed at room temperature.

## 3 Results and Discussion

### 3.1 TEM, HRTEM and XRD Characterization of mNPs@C

Figure 1A and b show TEM and HRTEM images of mNPs@C where crystalline particles coated with the amorphous phase of carbon can be clearly observed. Only one d-spacing value was identified, associated to magnetite. HRTEM studies reveal that the obtained sample is composed by an amorphous carbon matrix with embedded mNPs. Figure 1C shows a log-normal size distribution, with an average size of 20 nm. Additionally, the

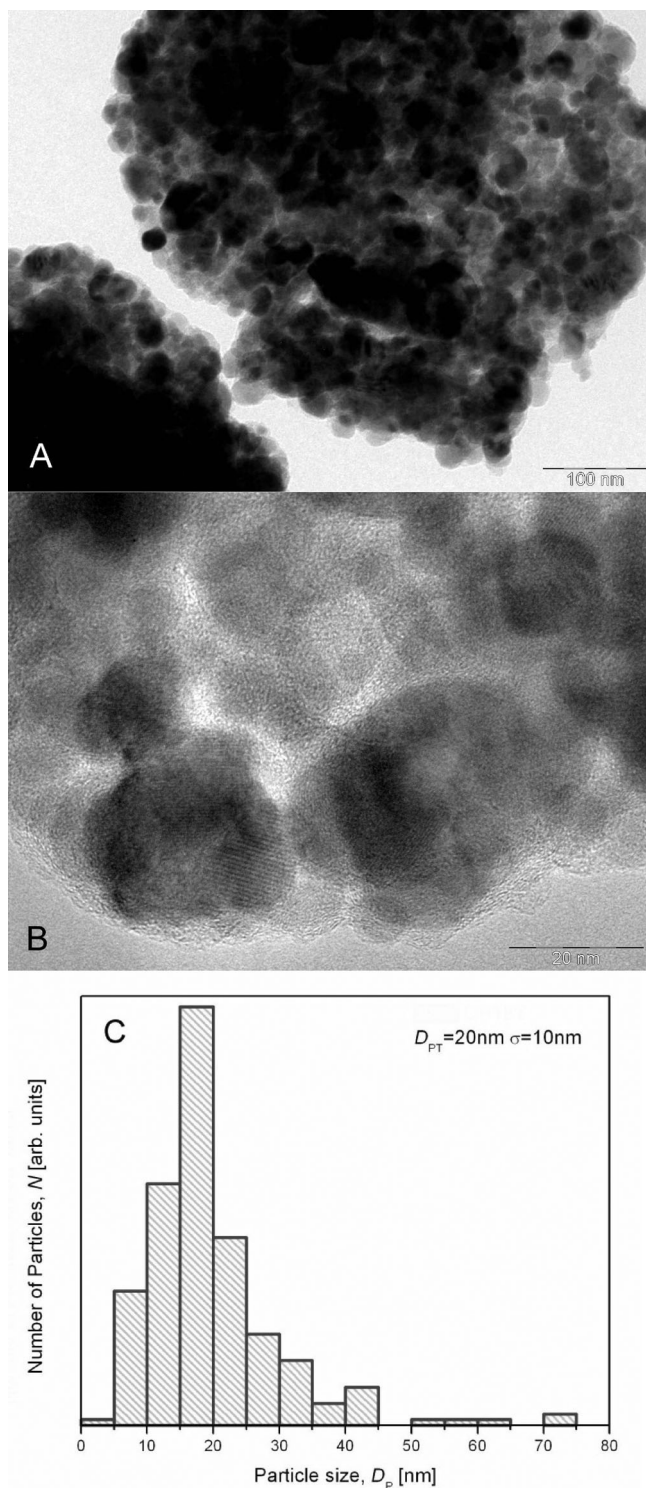


Fig. 1. TEM (A) and HRTEM (B) images of crystalline mNPs@C. (C) Log-normal size distribution, with an average size of 20 nm.

XRD pattern corresponding to mNPs@C reveals only reflections corresponding to magnetite, indicating that the crystalline material is single-phase [35]. Since carbon is an amorphous phase, these are not expected to come from this material. Moreover, it is important to remark

that mNPs@C can be prepared with high efficiency by a simple and inexpensive method such as mechanochemistry.

### 3.2 Electrochemical Characterization of mNPs@C/CPE

Magnetite NPs can be considered as an artificial biocatalyst due to the intrinsic peroxidase-like activity that they exhibit even under extreme reaction conditions [29]. In order to explore this concept and characterize the electrochemical behavior of mNPs@C, investigate their peroxidase-like catalytic activity and consider their application in biosensing strategies, a composite electrode material was modified accordingly with the obtained carbon-coated magnetic nanoparticles (Section 2.4).

For the evaluation of the electrocatalytic response towards  $0.010\text{ mol L}^{-1}$  hydrogen peroxide by cyclic voltammetry, three composite electrodes were assayed and compared: bare CPE (a), 5.0% w/w commercial magnetite microparticles (MPs)/CPE (b) and 5.0% w/w mNPs@C/CPE (c). As it is shown in Figure 2A, there is an important decrease in the overvoltage for the electrooxidation and mainly for the electroreduction of hydrogen peroxide and a significant increase of the associated currents for 5.0% mNPs@C/CPE, compared to the poor electrochemical response at the bare electrode (CPE) [26,31,36–38] and at 5.0% MPs/CPE [37].

At the 5.0% mNPs@C/CPE, the reduction current starts to increase at potentials more negative than 0.200 V, as expected according to the excellent electrocatalytic action of magnetite NPs towards the reduction of hydrogen peroxide [9,22,31]. It is important to remark that NPs also catalyze the hydrogen peroxide oxidation, starting at more positive potentials than 0.300 V, although this effect is less pronounced than in the case of the reduction. Thus, the preferential reduction of hydrogen peroxide at mNPs@C/CPE, allows reaching low-potential values for the amperometric detection, offering a good alternative for the selective enzymatic quantification of glucose. Therefore,  $-0.100\text{ V}$  was selected as working potential for further amperometric experiments. Figure 2B depicts cyclic voltammograms obtained for 0.010 M hydrogen peroxide at CPE containing increasing amounts of mNPs@C: 0.0 (a), 2.5 (b), 5.0 (c), 10.0 (d) and 20.0 (e) % w/w. As expected, there is an enhancement in the reduction currents for hydrogen peroxide with the amount of nanomaterial, whereas there is an important increase in the capacitive currents that can be seen more clearly at the 20.0% mNPs@C/CPE. A similar trend is observed for the 15.0% mNPs@C/CPE (not shown). This behavior is due to the nonconductive nature of magnetite and a resistive behavior due to a poor agglutination of the composite matrix with high content of NPs, as was reported previously [26].

The content of mNPs@C in the composite material proved to be a very critical parameter for the performance of the electrode. Figure 3A displays calibration plots obtained from amperometric recordings performed

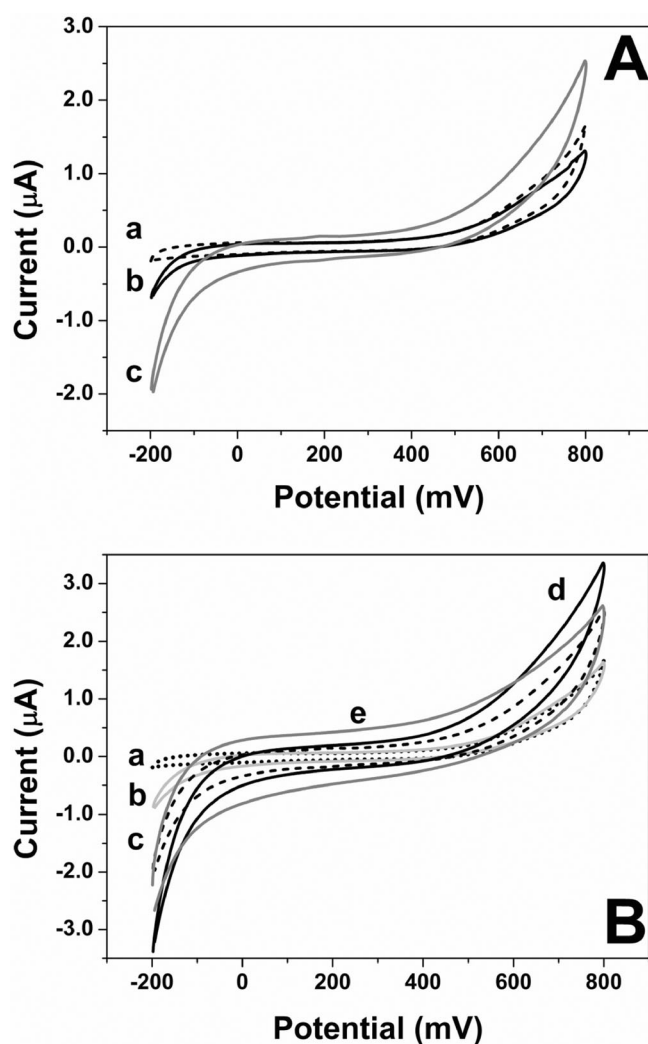


Fig. 2. (A) Cyclic voltammograms for  $0.010 \text{ mol L}^{-1}$  hydrogen peroxide at (a: dashed line) bare carbon paste electrode (CPE), at (b: solid black line) CPE modified with 5.0% w/w  $\text{Fe}_3\text{O}_4$  microparticles (5.0% MPs/CPE) and at (c: solid grey line) CPE modified with 5.0% w/w mNPs@C nanoparticles (5.0% NPs/CPE). Supporting electrolyte:  $0.050 \text{ mol L}^{-1}$  phosphate buffer solution pH 7.40. Scan rate:  $0.100 \text{ V s}^{-1}$ . (B) Cyclic voltammograms for  $0.010 \text{ mol L}^{-1}$  hydrogen peroxide at CPE containing different percentages w/w of mNPs@C: 0.0 (a: dotted line), 2.5 (b: light grey line), 5.0 (c: dashed line) 10.0 (d: solid black line) and 20.0 (e: solid grey line) % w/w NPs. Other conditions as in Figure 2A.

at  $-0.100 \text{ V}$  for successive additions of  $1.0 \times 10^{-3} \text{ mol L}^{-1}$  hydrogen peroxide at CPE containing different percentages of mNPs@C: 0.0 (a), 2.5 (b), 5.0 (c), 10.0 (d), 15.0 (e) and 20.0 (f) % w/w and 10.0 (g) % w/w uncoated-magnetite NPs, respectively. Figure 3B shows the corresponding sensitivity values towards hydrogen peroxide obtained from the calibration plots at  $-0.100 \text{ V}$  (shown in Figure 3A). The corresponding sensitivities are the following:  $(0.63 \pm 0.07)$ ,  $(11.7 \pm 0.5)$ ,  $(27 \pm 3)$ ,  $(44 \pm 3)$ ,  $(66 \pm 4)$  and  $(8 \pm 2) \times 10^1 \mu\text{A M}^{-1}$  for CPE containing 0.0; 2.5; 5.0; 10.0; 15.0 and 20.0% w/w mNPs@C, respectively; while

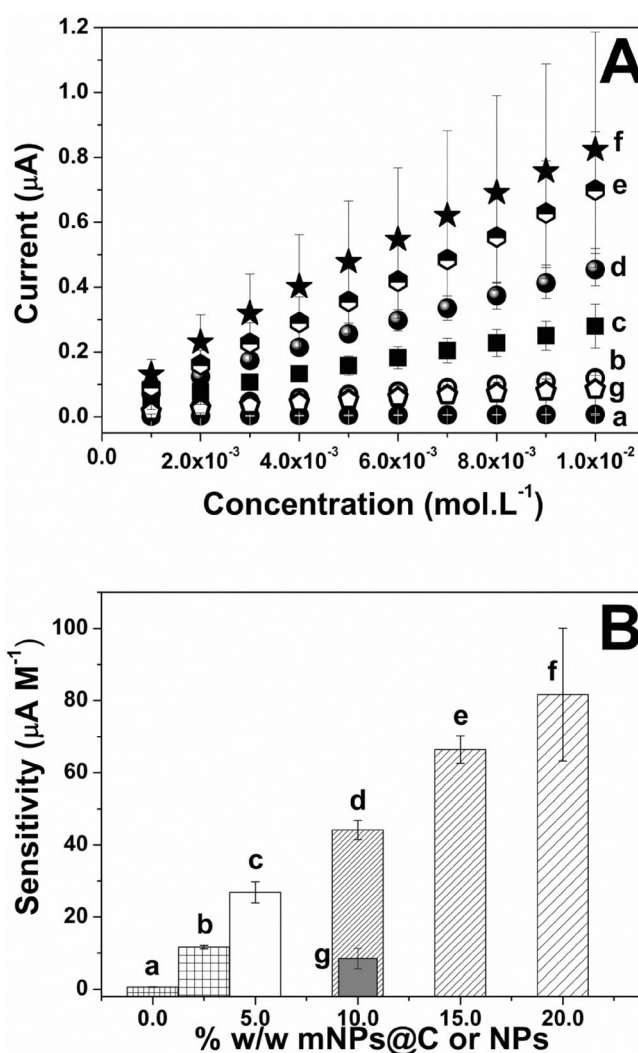


Fig. 3. (A) Calibration plots obtained from amperometric experiments for successive additions of  $1.0 \times 10^{-3} \text{ mol L}^{-1}$  hydrogen peroxide performed at  $-0.100 \text{ V}$  at CPE containing different percentages w/w of mNPs@C: 0.0 (a), 2.5 (b), 5.0 (c), 10.0 (d), 15.0 (e), 20.0 (f) % w/w and uncoated magnetite nanoparticles 10.0% w/w (g). Supporting electrolyte:  $0.050 \text{ mol L}^{-1}$  phosphate buffer solution pH 7.40. (B) Sensitivity towards hydrogen peroxide obtained from amperometric experiments shown in A at CPE containing different percentages w/w of mNPs@C: 0.0 (a), 2.5 (b), 5.0 (c), 10.0 (d), 15.0 (e), and 20.0 (f) % w/w and uncoated magnetite nanoparticles 10.0% w/w (g). Other conditions as in Figure 3A.

for 10.0% w/w uncoated magnetite NPs the sensitivity value found was  $(9 \pm 3) \mu\text{A M}^{-1}$ . Analyzing the sensitivity values for CPE containing increasing amounts of mNPs@C, a linear relationship is obtained (with regression coefficient  $R^2 = 0.998$ ). As it was previously concluded from the cyclic voltammetry experiments (Figure 2B), there is an important influence of the content of mNPs@C on the sensitivity towards hydrogen peroxide. However, for 15.0 and 20.0% mNPs@C/CPE, in addition to the important increase of the sensitivity, a very low reproducibility of the calibration curve is observed. This

fact could be attributed to the agglutination difficulty of the composite matrix with the increasing content of magnetite NPs [26]. In view of these results, a 10.0% w/w mNPs@C was selected as the optimum composition of the electrode material for a higher sensitive response. Likewise, the sensitivities towards hydrogen peroxide at 10.0% mNPs@C/CPE and 10.0% uncoated magnetite NPs/CPE were compared (Figure 3A, curve d; Figure 3A, curve g; Figure 3B, column d and Figure 3B, column g) under the same experimental conditions. The sensitivity obtained for mNPs@C is higher than the one for uncoated magnetite NPs by a factor of 5, demonstrating that the carbon surrounding provides a better environment for the catalytic activity and the electron transfer of mNPs@C.

In the development of electrochemical biosensing strategies for blood glucose determination, a very remarkable aspect to take into account is the interference of easily oxidizable compounds, usually present in biological fluids, such as ascorbic acid (AA) and uric acid (UA). For this purpose, the catalytic activity of mNPs@C/CPE towards the oxidation of these compounds was investigated. Figure 1SI (Supporting Information) shows the typical voltammetric profiles obtained at  $0.100 \text{ V s}^{-1}$  for  $1.0 \times 10^{-3} \text{ mol L}^{-1}$  AA (A) and for  $1.0 \times 10^{-3} \text{ mol L}^{-1}$  UA (B) at CPE (a–dotted line) and 10.0% mNPs@C/CPE (b–solid line). For mNPs@C/CPE, there is a negative shift of 46 mV in the oxidation peak potential for AA and a negligible increase in the peak current from 23.6 to 24.7  $\mu\text{A}$ . Moreover, for UA the catalytic effect is more evident, with a negative shift of 73 mV in the oxidation peak potential and an increase in the peak current from 12.5 to 21.6  $\mu\text{A}$  (1.7 times). Nevertheless, although mNPs@C reveal a slight catalysis for the oxidation of UA, the effect is not significant compared to the catalysis exhibited for hydrogen peroxide. Furthermore, at  $-0.100 \text{ V}$ , the selected potential for amperometric detection of hydrogen peroxide, there is no response to successive additions of AA and UA, even at higher concentrations than the physiological levels of these compounds (not shown), allowing a highly specific detection of hydrogen peroxide. Therefore, these results allow to conclude that mNPs@C/CPE constitute a highly efficient system for the electrocatalytic reduction of hydrogen peroxide, making it possible to consider its application in biosensing strategies for highly sensitive and selective glucose determination.

### 3.3 Design and Analytical Performance of GOx/mNPs@C/CPE

Upon the excellent performance of mNPs@C/CPE towards hydrogen peroxide reduction and the remarkable selectivity in amperometric experiments, the following step was the design of a glucose biosensor by modifying 10.0% mNPs@C/CPE with glucose oxidase (GOx) as biocatalyst. GOx catalyzes the oxidation of glucose to gluconic acid in presence of oxygen which is the natural regenerator of the enzyme active site, producing hydrogen

peroxide after GOx regeneration. The amount of GOx within the composite has demonstrated to be an important parameter in the development of the glucose biosensor, being this amount usually comprised between 5.0 and 10.0% [26,36]. It is important to notice that for excessive amounts of GOx, commonly higher than 10.0% w/w, the oxygen consumption becomes more important, producing a shortening of the linear range [26,38]. Therefore, 5.0% w/w GOx was selected in order to compare the proposed magnetite NPs modified composite electrode with previous by reported results [26]. In the designed biosensing strategy, the biosensor was obtained by dispersing 5.0% w/w of GOx within CPE modified with 10.0% w/w mNPs@C. The reduction current of the hydrogen peroxide produced during the step of GOx regeneration obtained at  $-0.100 \text{ V}$ , was taken as analytical signal. Figure 4A illustrates a current–time profile for successive additions of  $2.5 \times 10^{-4} \text{ mol L}^{-1}$  glucose, performed at  $-0.100 \text{ V}$  at 5.0% GOx/10.0% mNPs@C /CPE. A very

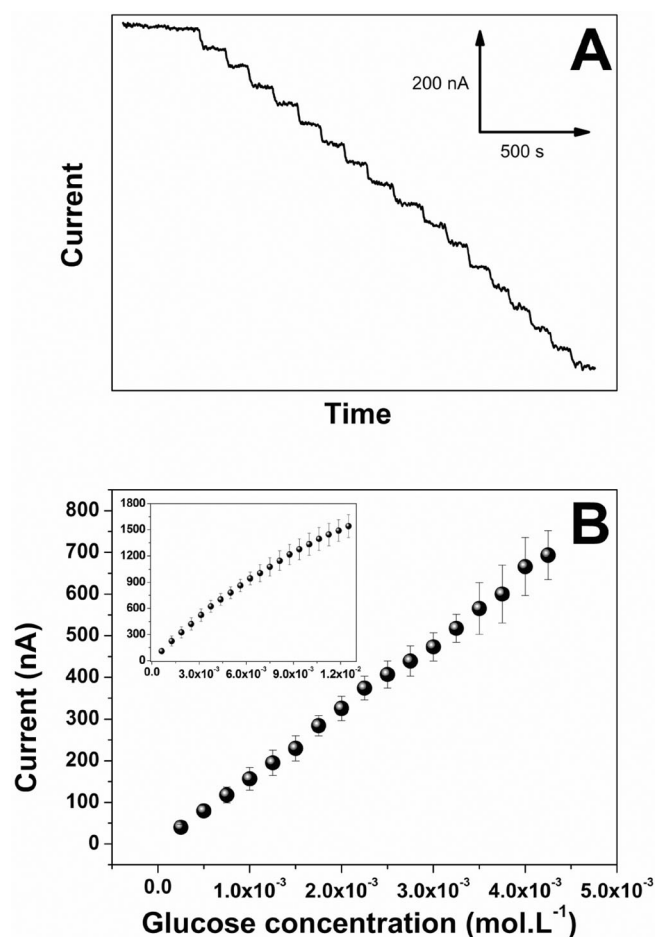


Fig. 4. (A) Amperometric recordings for successive additions of  $2.5 \times 10^{-4} \text{ mol L}^{-1}$  glucose performed at  $-0.100 \text{ V}$  at CPE containing 10.0% w/w mNPs@C and 5.0% w/w GOx (10.0% mNPs@C/5.0% GOx/CPE). (B) Calibration plot obtained from the amperometric recordings (shown in A). Inset: Calibration plot for successive additions of  $6.25 \times 10^{-4} \text{ mol L}^{-1}$  glucose in an extended range of concentrations. Other conditions as in Figure 3.

fast and well-defined response is observed for each glucose addition. Amperometric experiments for five separate additions of 5.0 mM (0.90 g/dL) glucose were carried out in order to determine the response time of the biosensor. It was found that  $(11 \pm 1)$  s is the necessary time to reach 90% of the steady-state current. Thus, the response time of the biosensor is comparable to those of the commercially available "point-of-care" (POC) devices. Similar amperometric experiments performed at 5.0% GOx/CPE at  $-0.100$  V gave no response, as expected, due to the poor reduction of the hydrogen peroxide enzymatically generated at bare CPE [36]. Figure 4B displays a calibration plot obtained from the current–time profile (shown in Figure 4A) while the inset shows a calibration curve for successive additions of  $6.25 \times 10^{-4}$  mol L $^{-1}$  glucose performed at  $-0.100$  V in an extended range of glucose concentration. A linear relationship between current and glucose concentration is obtained up to  $7.5 \times 10^{-3}$  mol L $^{-1}$  glucose (135 mg/dL), comprising the entirely physiological range and incipient pathological values. For higher glucose concentrations, the current increases non-linearly, as expected for biocatalyzed reactions. The average sensitivity obtained at  $-0.100$  V was  $(1.62 \pm 0.05) \times 10^5$  nA L mol $^{-1}$  (correlation coefficient  $R^2 = 0.9992$ ). The detection limit, calculated as  $3.3 (\sigma/S)$  where  $\sigma$  is the ten blank standard deviation and  $S$  is the sensitivity of the calibration curve, was  $2.0 \times 10^{-6}$  M, while the quantification limit calculated as  $10 (\sigma/S)$  was  $6.1 \times 10^{-6}$  mol L $^{-1}$ . The enzyme immobilization process usually alters the microenvironment of the enzyme active site. This might affect the intrinsic characteristics of the enzyme. The kinetics parameters of the bioelectrode,  $K_M^{\text{app}}$  and  $I_{\text{max}}$ , were calculated by the Eadie–Hofstee plot obtained from the data of the calibration plot shown in Figure 4B (inset). The values obtained were the following:  $K_M^{\text{app}}$ :  $(0.02298 \pm 0.0004)$  mol L $^{-1}$  and  $I_{\text{max}}$ :  $(4.39 \pm 0.06) \times 10^3$  nA. The value found for the  $K_M^{\text{app}}$  falls within the range reported for  $K_M$  of GOx in homogeneous solution [39] and in the composite ceramic carbon matrix ( $K_M^{\text{app}}$   $0.020 \pm 0.002$  mol L $^{-1}$ ) [40], suggesting that the en-

vironment provided by mNPs@C/composite matrix where GOx was immobilized is suitable for the biocatalytic activity of the enzyme and does not alter the microenvironment of the GOx active site.

Neither highly hydrophobic nor totally hydrophilic electrode matrices are desirable for sensing applications. In a hydrophobic environment, the analyte cannot approach the embedded enzyme, however a hydrophilic environment exhibits a large background current [40–42]. In the hydrophobic environment of a CPE matrix the enzyme could alter its conformation in order to expose the hydrophobic residues and consequently its active site could be more or less accessible to the diffusion of the analytes. Likewise, the diffusion of analytes towards the catalytic nanomaterial also could be affected by the hydrophobic environment. The main factor that clearly reflects the diffusion problems in an amperometric biosensor is the change in the speed of the response. As it was widely documented [26,27,43,44] several strategies have been proposed for the development of enzymatic glucose biosensors based on modified nanomaterials-CPE, where is clearly demonstrated that the stationary currents are reached in few seconds, proving that diffusion problems could be overcome even in a surrounding hydrophobic environment. In addition, the determination of kinetic parameters of the proposed biosensing strategy confirmed that the hydrophobic environment does not affect significantly the affinity of the immobilized enzyme by its substrate. It is important to remark that in some cases the  $K_M^{\text{app}}$  value of the bioelectrode is even smaller than the one of the enzyme in solution [43], evidencing the increase of the enzymatic affinity towards its substrate.

The easily renewable surface, among other advantages, is one of the most prominent features exhibited by composite carbon paste electrodes. This attribute, coupled to the miniaturization processes and the advantages of nanomaterials, make these kind of composites feasible tools as one-shot sensing devices, widely suitable for decentralized determinations of blood glucose level [24,25]. However, in order to determine another important analytical pa-

Table 1. Comparison of performance of different electrochemical glucose biosensors based on magnetite or iron nanoparticles. GOx/GOD: glucose oxidase; Fe $_3$ O $_4$ : magnetite nanoparticles electrochemically synthesized; Fe: acicular iron nanoparticles obtained from thermal reduction of acicular goethite nanoparticles; Fe $_3$ O $_4$ @SiO $_2$ : SiO $_2$  coated magnetite nanoparticles; mNPs@C: C-coated magnetite nanoparticles; BQ: 1,4-benzoquinone; CPE: Carbon paste electrode; CPEE: enzymatic (GOD) carbon paste electrode; MWNTs: multiwalled carbon nanotubes; GC: glassy carbon electrodes.

Glucose biosensor	Linear range (mol L $^{-1}$ )	Sensitivity (nA L mol $^{-1}$ )	Long-term stability	$R^2$	Detection limit (M)	Ref.
GOx-Fe $_3$ O $_4$ -CPE	$1.0 \times 10^{-3}$ – $8.0 \times 10^{-3}$	$(3.2 \pm 0.4) \times 10^4$	90% after 10 months stored at 4 °C	Not available	$3.0 \times 10^{-4}$	[26]
GOx-Fe-CPE	$5.0 \times 10^{-4}$ – $2.0 \times 10^{-2}$	$(8.8 \pm 0.5) \times 10^3$	91% after 140 days stored at 4 °C	Not available	$2.0 \times 10^{-4}$	[27]
BQ-Fe $_3$ O $_4$ -CPEE	$1.9 \times 10^{-8}$ – $3.1 \times 10^{-6}$	$1.66 \times 10^9$	Not available	0.975	$1.9 \times 10^{-7}$	[31]
GOD/Fe $_3$ O $_4$ @SiO $_2$ /MWNTs/GC	$1 \times 10^{-6}$ – $3.0 \times 10^{-2}$	Not available	Not available	0.99994	$8 \times 10^{-7}$	[32]
GOx/mNPs@C/CPE	$1.25 \times 10^{-4}$ – $7.5 \times 10^{-3}$	$(1.62 \pm 0.05) \times 10^5$	100% after 100 days stored at 4 °C	0.9992	$2.0 \times 10^{-6}$	This work

parameter for practical sensing applications, we examined the short-term and long-term stability of GOx/mNPs@C/CPE evaluating the sensitivity of amperometric assays for glucose. The short-term stability of the composite demonstrated to be excellent, since the *RSD* for 10 successive amperometric assays for glucose performed at  $-0.100$  V was 1.2% (not shown). The sensitivity along 15 days of periodic use for amperometric assays at  $-0.100$  V remained constant. GOx-mNPs@C was stored at  $4^{\circ}\text{C}$  after every set of experiments. The long-term stability was evaluated from the sensitivity of the amperometric calibration curves at  $-0.100$  V for GOx-mNPs@C-modified composite matrix. The response of the biosensor remained in 100% after 100 days from the date of preparation and first test, demonstrating a noteworthy long-term stability. These results suggest that mNPs@C/CPE provide an adequate microenvironment that preserves the biocatalytic activity of GOx. A further comparison of the performance of different electrochemical glucose biosensors modified with magnetite or iron nanoparticles as catalytic element was summarized in Table 1.

The biosensor was further challenged by the addition of AA and UA. Figure 5 depicts the current – time profile at  $-0.100$  V obtained after one addition of  $5.0 \times 10^{-4} \text{ mol L}^{-1}$  glucose, followed by successive additions of  $2.0 \times 10^{-5} \text{ mol L}^{-1}$  AA (a) and  $4.0 \times 10^{-5} \text{ mol L}^{-1}$  UA (b) up to achieve final concentrations of  $2.0 \times 10^{-4} \text{ mol L}^{-1}$  and  $4.0 \times 10^{-4} \text{ mol L}^{-1}$ , respectively. No interference signal in the presence of glucose was revealed for such concentrations, which are even higher than the maximum physiological levels found in human blood serum. This fact evidences the advantages of the preferential electrocatalytic detection of the enzymatically generated hydrogen

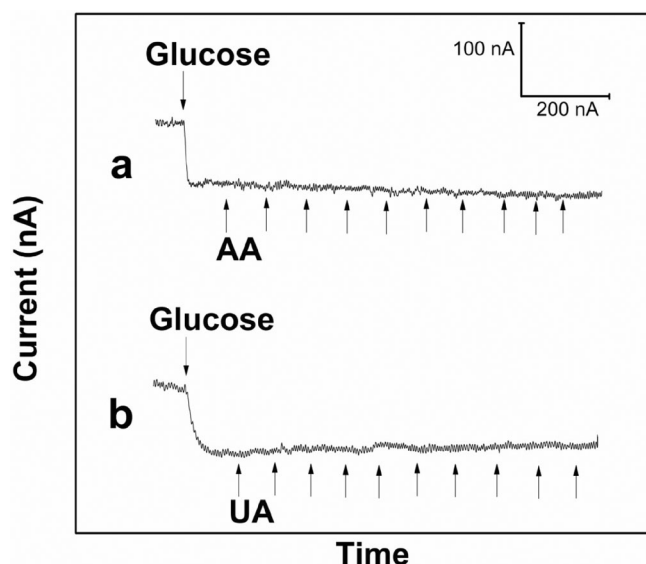


Fig. 5. Current – time profiles performed at 10.0% mNPs@C/5.0%GOx/CPE) for an addition of  $5.0 \times 10^{-4} \text{ mol L}^{-1}$  glucose and successive additions of (a)  $2.0 \times 10^{-5} \text{ mol L}^{-1}$  AA (up to reach a final concentration of  $2.0 \times 10^{-4} \text{ mol L}^{-1}$ ) and (b)  $4.0 \times 10^{-5} \text{ mol L}^{-1}$  UA (up to reach a final concentration of  $4.0 \times 10^{-4} \text{ mol L}^{-1}$ ). Other conditions as in Figure 3.

peroxide, leading to a high sensitivity and an excellent selectivity.

In order to evaluate the applicability of the bioelectrode for glucose practical determinations, 5.0% GOx/10.0% mNPs@C/CPE was further challenged with human blood serum samples (Standatrol S-E-2, levels physiological N1 and pathological N2, Wiener Lab.). The glucose concentration obtained in the sample after 5 determinations were  $(91.6 \pm 0.4) \text{ mg/dL}$  for level N1 and  $(232 \pm 6) \text{ mg/dL}$  for level N2, while the glucose concentration reported by Wiener for levels N1 and N2 were 89 mg/dL and 238 mg/dL, respectively. These values gave a relative error of +2.8% and  $-2.6\%$  for N1 and N2 samples, respectively, indicating the noteworthy performance of the proposed glucose biosensor for practical assays.

## 4 Conclusions

The use of mNPs@C for the development of an electrochemical glucose biosensor was proposed for the first time. mNPs@C demonstrated an excellent catalytic activity towards hydrogen peroxide enzymatically generated. This feature allowed quantifying glucose at potentials negative enough to avoid the interference of a large excess of easily oxidizable compounds or complex matrices as human blood serum. The resulting bioelectrode demonstrated an outstanding analytical performance, comparable and even better than previous works using magnetite nanoparticles. The simplicity of the preparation, the high sensitivity and selectivity, the excellent reproducibility of the proposed biosensor, and the noteworthy correlation of the results for blood human serum with those obtained using the spectrophotometric method, convert the proposed biosensor in a very good promise for practical applications in real biological samples. To our knowledge, this is the first example of using carbon-coated magnetite NPs for the development of an amperometric biosensor with an improved and highly selective glucose detection taking advantages of their intrinsic peroxidase-like activity. Based on the catalytic activity of mNPs@C and their known possibilities of functionalization, it is expected that the surface modification of these nanoparticles with biomolecules will allow obtaining very efficient biosensors for a wide range of biomolecules.

## Acknowledgements

The authors thank CONICET, SECyT-UNC, ANPCyT, for the financial support. M. A. and C. S. T. acknowledge the CONICET fellowship. Authors gratefully acknowledge Dr. Gustavo A. Rivas and Dr. María D. Rubianes for fruitful discussions.

## References

- [1] S. Kumar, S. Kumar, M. A. Ali, P. Anand, V. V. Agrawal, R. John, S. Maji, B. D. Malhotra, *Biotechnol. J.* **2013**, *8*, 1267.

- [2] E. P. Cicolatti, M. J. A. Silva, M. Kleina, V. Feddern, M. M. C. Feltes, J. V. Oliveira, J. L. Ninowa, D. de Oliveira, *J. Mol. Catal. B, Enzym.* **2014**, *99*, 56.
- [3] M. A. Syed, *Biosens. Bioelectron.* **2014**, *51*, 391.
- [4] J. Kirsch, C. Siltanen, Q. Zhou, A. Revzin, A. Simonian, *Chem. Soc. Rev.* **2013**, *42*, 8733.
- [5] S. Kruss, A. J. Hilmer, J. Zhang, N. F. Reuel, B. Mu, M. S. Strano, *Adv. Drug Deliver. Rev.* **2013**, *65*, 1933.
- [6] K. V. Ragavana, M. K. Rastogi, M. S. Thakur, *TrAC* **2013**, *52*, 248.
- [7] P. D'Orazio, *Clin. Chim. Acta* **2011**, *412*, 1749.
- [8] Y. W. Chu, D. A. Engebretson, J. R. Carey, *J. Biomed. Nanotech.* **2013**, *9*, 1951.
- [9] L. Shanhu, L. Feng, X. Ruimin, Z. Jun-Jie, *Chem. A Eur. J.* **2011**, *17*, 620.
- [10] C. Albornoz, E. E. Sileo, S. E. Jacobo, *Phys. B* **2004**, *354*, 149.
- [11] C. Albornoz, S. E. Jacobo, *J. Magn. Magn. Mater.* **2006**, *305*, 12.
- [12] N. J. François, S. Allo, S. E. Jacobo, M. E. Daraio, *J. Appl. Polym. Sci.* **2007**, *105*, 647.
- [13] P. E. Podzus, M. E. Daraio, S. E. Jacobo, *Phys. B* **2009**, *404*, 2710.
- [14] J. C. Apesteguy, S. E. Jacobo, N. N. Schegoleva, G. V. Kuryanskaya, *J. Alloy. Compd.* **2010**, *495*, 509.
- [15] P. Bertoglio, S. E. Jacobo, M. E. Daraio, *J. Appl. Polym. Sci.* **2010**, *115*, 1859.
- [16] Z. Ai-Xian, C. Zhong-Xiao, W. Jin-Ru, L. Juan, Y. Huang-Hao, C. Guo-Nan, *Biosens. Bioelectron.* **2013**, *49*, 519.
- [17] Z. Chen, J. J. Yin, Y. T. Zhou, Y. Zhang, L. Song, M. Song, S. Hu, N. Gu, *ACS Nano* **2012**, *6*, 4001.
- [18] L. Cheng-Hao, Y. Cheng-Ju, T. Wei-Lung, *Anal. Chim. Acta* **2012**, *745*, 143.
- [19] L. Jianbo, H. Xiaona, H. Shuai, W. Tao, L. Wenqi, Z. Xing, Y. Jun-Jie, W. Xiaochun, *Sens. Actuators B* **2012**, *166–167*, 708.
- [20] M. Patila I. V. Pavlidis, E. K. Diamanti, P. Katapodis, D. Gournis, H. Stamatis, *Process Biochem.* **2013**, *48*, 1010.
- [21] H. Teymourian, A. Salimi, S. Khezrian, *Biosens. Bioelectron.* **2013**, *49*, 1.
- [22] N. Xiaoying, X. Yinyin, D. Yalei, Q. Liye, Q. Shengda, C. Hongli, C. Xingguo, *J. Alloy. Compd.* **2014**, *587*, 74.
- [23] L. C. Clark, C. Lyons, *Ann. NY. Acad. Sci.* **1962**, *102*, 29.
- [24] J. Wang, *Talanta* **2008**, *75*, 636.
- [25] V. Scognamiglio, *Biosens. Bioelectron.* **2013**, *47*, 12.
- [26] F. N. Comba, M. D. Rubianes, L. Cabrera, S. Gutiérrez, P. Herrasti, G. A. Rivas, *Electroanalysis* **2010**, *22*, 1566.
- [27] F. N. Comba, M. D. Rubianes, P. Herrasti, G. A. Rivas, *Sens. Actuators B* **2010**, *149*, 306.
- [28] F. N. Comba, F. Gutiérrez, P. Herrasti, M. D. Rubianes, G. A. Rivas, *Electroanalysis* **2012**, *24*, 1541.
- [29] S. Liu, F. Lu, R. Xing, J. Zhu, *Chem. Eur. J.* **2011**, *17*, 620.
- [30] M. Eguílaz, R. Villalonga, P. Yáñez-Sedeño, J. M. Pingarrón, *Anal. Chem.* **2011**, *83*, 7807.
- [31] P. E. Erden, B. Zeybek, Ş. Pekyardımcı, E. Kılı, Artif, *Cells, Nanomed. Biotech.* **2013**, *41*, 165.
- [32] T. T. Baby, S. Ramaprabhu, *Talanta* **2010**, *80*, 2016.
- [33] R. Liang, G. Yao, L. Fan, J. Qiu, *Anal. Chim. Acta* **2012**, *737*, 22.
- [34] X. Ge, W. Zhang, Y. Lin, D. Du, *Biosens. Bioelectron.* **2013**, *50*, 486.
- [35] M. Arana, S. E. Jacobo, H. Troiani, P. G. Bercoff, *IEEE T. Magn.* **2013**, *49*, 4547.
- [36] M. C. Rodríguez, G. A. Rivas, *Electroanalysis* **2001**, *13*, 1179.
- [37] M. S. Lin, H. J. Leu, *Electroanalysis* **2005**, *17*, 2068.
- [38] G. L. Luque, M. C. Rodríguez, G. A. Rivas, *Talanta* **2005**, *66*, 467.
- [39] R. A. Kamin, G. S. Wilson, *Anal. Chem.* **1980**, *52*, 1198.
- [40] S. Sampath, O. Lev, *Anal. Chem.* **1996**, *68*, 2015.
- [41] I. Svancara, K. Vytras, K. Kalcher, A. Walcarus, J. Wang, *Electroanalysis* **2009**, *21*, 7.
- [42] A. L. Kavitha, H. Gurumallesh Prabu, S. Ananda Babu, S. K. Suja, *J. Nanosci. Nanotech.* **2013**, *13*, 98.
- [43] J. Liu, F. Lu, J. Wang, *Electrochem. Commun.* **1999**, *1*, 341.
- [44] H.-P. Peng, R.-P. Liang, L. Zhang, J.-D. Qiu, *Biosens. Bioelectron.* **2013**, *42*, 293.

Received: April 4, 2014

Accepted: May 18, 2014

Published online: July 16, 2014